Characterization of Ultra Thin Films and Solid Surfaces by High Resolution Electron Energy Loss Spectroscopy

Chuhei Oshima

Department of Applied Physics, Waseda University, Okubo 4-3-1, Shinjyuku, Tokyo 169, Japan

(Received: Jan. 31, 1997 Accepted: Feb. 28, 1997)

Abstract

We have reviewed the recent data of HREELS. Slow electrons interact strongly with the dipole fields of FK modes at compound surfaces of either semiconductors or insulators, which produce large loss peaks. From the analysis of the FK mode, we have derived the atomic structure of Al_2O_3 thin layer and its thickness. We have demonstrated that the HREELS is a unique tool to search the high frequency phonons of graphite, h-BN and LaB_6. The phonon dispersion curves of thin films and surfaces provide a large amount of information on chemical bonding and deformation of the surface lattice.

1. Introduction

High resolution electron energy loss spectroscopy (HREELS) is one of the most powerful techniques to detect the atomic vibrations at solid surfaces. At present, it is used widely in various research fields such as chemical reactions, surface dielectric response and lattice dynamics near the surfaces. From the vibrational energies, chemisorbed molecules, chemisorbed species, and chemisorbed sites are discussed, which results in clarifying the reaction activity of solid surfaces [1]. The lattice-dynamical calculations of observed dispersion relation of surface phonons provides information about lattice dynamical parameters at the surfaces. Here, I will point out two peculiar features of this technique, and show a few examples mainly obtained in my laboratory in this review.

(1) Since an electron is a charged particle, it interacts with longitudinal electric fields excited by atomic vibrations, phonons and the other excitations. From two different scattering mechanisms, dipole and impact scattering, we can assign the vibrational modes of observed phonons [1]. From the observed spectra, we can derive the thickness of the insulating thin film, dielectric functions, and qualitative information about the electron spatial distributions at surfaces. In the next paragraph, I will show new data concerning ultra-thin films of alumina, graphite and hexagonal boron nitride (h-BN). In addition, the dispersion curves determined by off-specular spectra through impact scattering indicate deformation of the surface lattice of lanthanum hexaboride.

(2) In general, slow electrons below a few hundred eV used in HREELS have the most suitable conditions of both the momentum and the energy for one-phonon excitations with high-frequency modes. By utilizing the excitation process, we can determine the phonon dispersion relation. On the other hand, the other techniques can detect only a part of surface phonon dispersion. Namely, He atom scattering and neutron scattering are limited for their measurable vibrational energy less than a few ten meV [2], because of their large mass in comparison with the electron mass, while only the vibrational modes at the long-wave limit can be measured by optical methods such as infra-red absorption spectroscopy, Raman spectroscopy and sum frequency spectroscopy. Namely, the HREELS is only one way to determine whole dispersion curves of the high frequency phonons over the Brillouin zone of attractive materials such as diamond, carbide, oxide, and hydride. It should be noted that the full phonon dispersion of graphite and LaB_6 was determined in the two dimensional Brillouin zone by HREELS [3], which I will discuss later.

2. Experimental Apparatus

As shown in Fig.1, the EELS spectrometer used in this experiment is composed of an electron gun, a pre-monochromator, a main monochromator, acceleration lens, scattering chamber, deacceleration lens, a main analyzer, a post analyzer and an electron detector. The electrons emitted by the electron gun are monochromatized by the tandem electrostatic

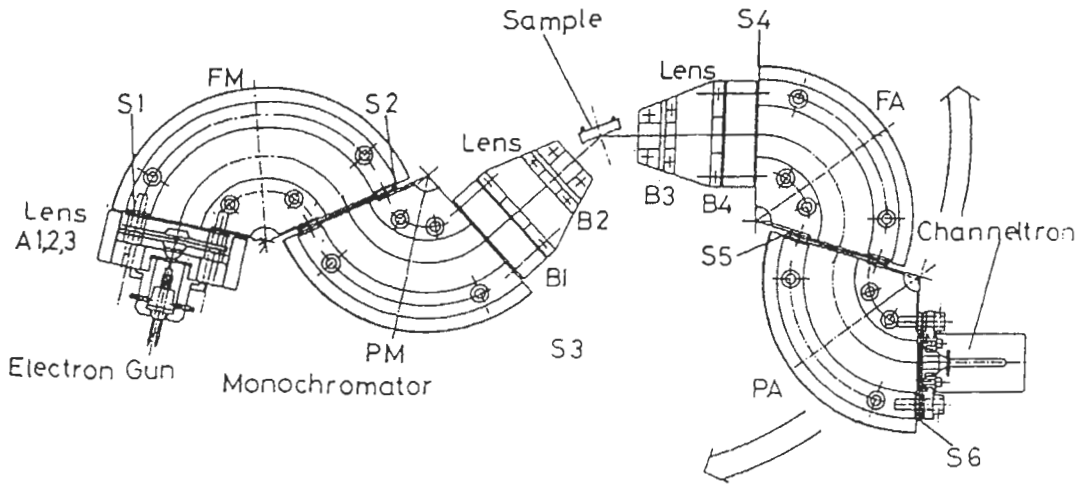

Fig. 1 A schematic representation of the high resolution electron energy loss spectrometer

energy selector, and are focused onto the specimen by the lens system. The scattered electrons are analyzed by the tandem energy analyzer and are detected by the channeltron. The energy resolution of ~ 1 meV was realized in the energy range of primary electrons from 1eV to 100 eV in our apparatus [4], and the better resolution of ~0.6 meV was reported by a new type of spectrometers [5,6]. For the measurement of the angle resolved HREEL spectra, the tandem. energy analyzer is rotated around the specimen. The wave vector $q_{//}$ of the exited surface phonons was determined from the momentum conservation law parallel to the surface as follows.

$$\boldsymbol{K}_{s//} - \boldsymbol{K}_{i//} = \boldsymbol{q}_{//} - \boldsymbol{G}_{//} \qquad (1)$$

Here, the vectors $\boldsymbol{K}_{s//}$ and $\boldsymbol{K}_{i//}$ are wave vectors of the scattered electrons and the incident electrons, respectively. The symbol // stands for the parallel component of each vectors to the surface. The wave vectors of the excited phonons (the reciprocal lattice vector) are denoted by $\boldsymbol{q}_{//}$ ($\boldsymbol{G}_{//}$). By plotting the observed loss energy *versus* the wave vector, we obtained the energy dispersion relation of the surface phonons, which appears in the bulk energy gaps [2]. Because of the strong localization of the vibrational amplitude of the surface phonons in the surface region, the dispersion of the surface phonons are considerably sensitive to changes in the chemical bond strength, electronic states and atomic structures.

3. Fuchs-Kliewer (FK) Modes

At both the compound surfaces of semiconductor and insulator, Fuchs-Kliewer (FK) mode is excited by slow electrons, which is sometimes called the surface phonon polariton appearing in the gaps of bulk polariton bands [1]. Their vibrational amplitudes are distributed around the surface region of ~10nm, and their longitudinal dipole fields extending both into the vacuum and interior of solid surfaces interact strongly with the slow electrons. Figure 2 shows a typical specular HREEL spectrum for the LiF(100) surface. Several large peaks appeared at each energy interval 71 meV in the spectrum. The 6 loss peaks on the left side of the elastic peak (3 gain peaks on the right) are attributed to the excitation (de-excitation) of the FK mode and their harmonics. In Fig.2, we observed other peaks indicated by arrows, which have been assigned to the edge mode of the surface polariton [7]. From the angle resolved HREEL spectra, the dispersion curves of the surface phonons have been determined as illustrated in Fig.3. The experimental data points are indicated by the filled circles. We observed two vibrational branches along the ΓX and ΓM directions. Many dotted curves in Fig.3

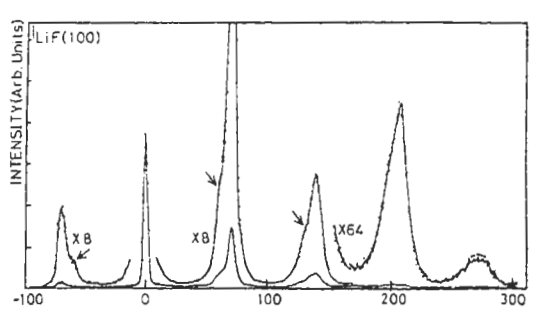

Fig. 2 A typical specular HREEL spectrum of LiF(100) surface.

correspond to the bulk phonon bands projected on the two-dimensional Brillouin zone of the (100) surface [8], which are calculated based on the slab model. Some solid curves in Fig.3 exhibits theoretical curves of the surface phonons calculated on the basis of the shell model [9]. In Fig.3, SP^+ stands for the parallel polarization of Li^+ ion in the sagittal plane mode and SH^- expresses the shear horizontal polarization of F^- ions. Those dispersion curves of surface phonons together with the theoretical calculation suggest that the shell charge of the F^- ions at the topmost layer is reduced by 4.5% from the bulk value [9].

Next, we will show the example of FK modes of the oxide thin layer on NiAl(100) indicating a (2×1) atomic structure. Figure 4 exhibits the specular HREEL spectrum of the oxide layer on NiAl(100) reported by Grassmann at al. [10]. In addition to the main loss peaks at 52 (ν_1), 75 (ν_2) and 112 (ν_3) meV, multiple loss peaks appear at 158.6 meV ($\nu_3 + \nu_1$), 180 meV ($\nu_3 + \nu_2$), and at 223.5 meV ($\nu_3 + \nu_3$). This spectrum resembles spectra taken from thin Al_2O_3 films on Al(111). From those data together with the dielectric theory, θ - Al_2O_3 monoclinic structure of the oxide films was assigned. The lattice constant of θ -Al_2O_3 layer explains very well the observed (2×1) LEED pattern of the film. The misfit amounts only to 2.5 % in one direction, and even to 1% in the other. The thickness of the oxide model, ~1.2nm can be estimated by comparing the normalized intensities. This is about the height of one unit cell of θ - Al_2O_3. Figure 5 shows a real space model for the suggested θ - Al_2O_3/ NiAl(001) atomic structure. The (2 × 1) atomic structure is seen clearly on this surface model. The model shows a crystal layer corresponding to 1.18nm and it exhibits that the (110) plane of the oxygen fcc lattice is perpendicular to the NiAl(001) and parallel to the NiAl[100] direction.

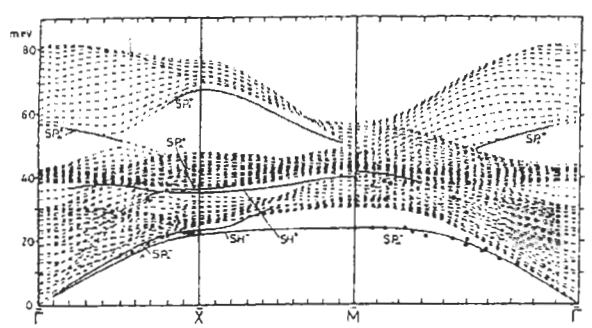

Fig. 3 The observed and theoretical phonon dispersion of LiF (100).

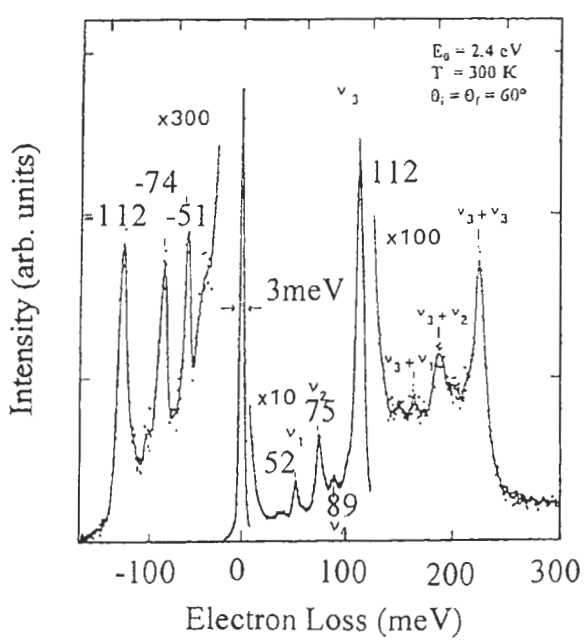

Fig. 4 A specular HREEL spectrum of the oxide NiAl(100) surface. The dielectric theory estimated the oxide thickness of 12 nm.

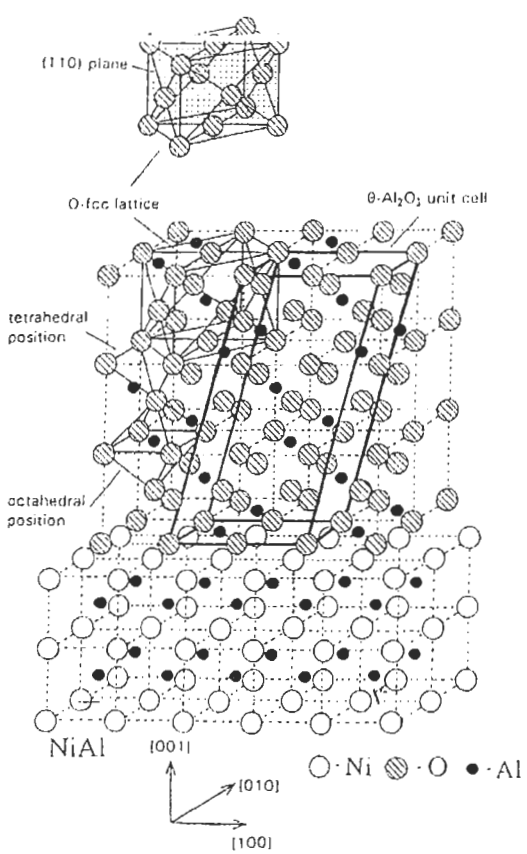

Fig. 5 The proposed atomic structure of θ - Al_2O_3layer on NiAl (100).

4. Monolayer Epitaxial Films of Graphite and h-BN [11]

A feature of graphite and h-BN is its layered structure with strong bonding in the basal plane and much weaker van der Waals interaction between the planes. As a results, the phonon spectra of their compounds cover a very wide energy range. The strong intraplanar bonds and the light atomic weights cause some vibrational energies up to 200 meV. While the weak interplanar bonding produces optical modes of very low vibrational energies. Figure 6 (a) shows the dispersion curves of graphite and monolayer graphite along the ΓM direction of the two-dimensional Brillouin zone[3]. The data points of graphite are indicated by (solid) circles. The open squares in the low-energy region represent the data points of neutron scattering [12]. It should be noted that the present curves connect smoothly to the dispersion curves of the bulk phonons: The extrapolated energies of two high frequency optical branches agreed with the optical bulk values, which are located at 196.9 and 106.9 meV at the Γ point [13]. Because of the two-dimensional character of the graphite, the observed dispersion curves agree with the bulk phonon curve with neutron scattering and an optical method. This is the first whole phonon dispersion of the graphite, which is now used widely as the reference data in the theoretical analysis of new carbon system of C_{60} metal alloy, carbon nanotubes, c-BN, and BNC_2.

Figure 6 (b) shows the phonon dispersion curves of a graphite film with one atomic-layer thickness formed on TaC(111) surface. We called it monolayer graphite (MG) hereafter. Observed 6 branches, (ZA, SH, LA, ZO and LO) were assigned as follows: The branch ZA is an acoustical mode, in which carbon atoms vibrate vertically to the film, and the branch ZO is an optical mode with perpendicular displacement. These modes deviate considerably from the bulk ones. The LA (LO) branch is longitudinal- acoustical (optical) mode. In these modes, carbon atoms vibrate laterally to the film, and the influence of the interfacial interaction is smaller than for the ZO and ZA modes with perpendicular polarization. In order to estimate the strength of the interfacial interaction, and the softening of the intra-layer forces, the phonon dispersion of the monolayer graphite lattice was calculated along the ΓM direction on the basis of a force constant model. The calculations indicate a

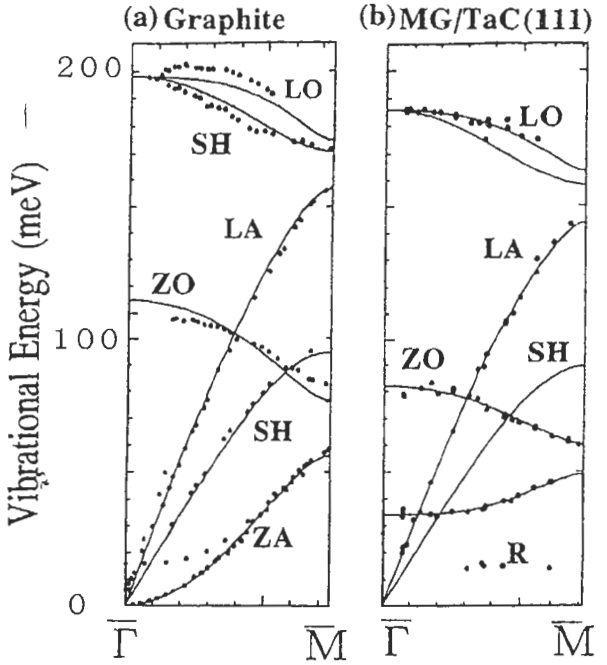

Fig. 6 (a) The experimental and theoretical dispersion curves of graphite surface and (b) monolayer graphite (MG)/ TaC(111).

~50% reduction of three-body force constants, and on the contrary, small changes in the stretching force constants between the first- and the second-nearest neighbors [14]. The observed changes in phonon dispersion are much correlated with the other following properties;

(a) The in-plane lattice expansion of ~ 3% shows weakening of the C-C bonds in MG.

(b) Theπbranch of MG shifts deeper from the bulk position by 1 eV.

(c) The relatively low work function of MG suggests that some part of the π electrons flow from the vacuum side to the interfacial side of MG.

The orbital mixing of π electrons with the d electrons of Ta atoms is the origin of the softening of graphite lattice and stiffening interfacial bonds [11]. Similar phonon dispersion was measured for monolayer epitaxial films of hexagonal boron nitride on Ni, Pd and Pt (111) surfaces [15,16]. The observed dispersion exhibits energy gaps at the two cross points of TO and LA(TA) branches. This is clear experimental evidence of the rumpling structure of the h-BN. The rumpling amplitude was estimated to be 0.018nm from intensity analysis of low energy electron diffraction [17].

5. Deformation of Surface Lattice [18,19]

Lanthanum hexaboride (LaB_6) is widely used as a long-life electron emitter with high brightness, because of its low work function (~ 2.6 eV) and a high melting point (~24000°C). The crystal structure of LaB_6 as shown in Fig.7, consists of octahedra of 6 boron atoms forming a cubie, making strong covalent bonds, while a La atom is locate at the center of this cubic. Two electrons transfer from a La atom to the three-dimensional framework of boron in the bulk. The high melting point of this compound and its high hardness originate from the three dimensional framework of boron, while the emission property largely depend on the electronic states of La atoms. At the clean (100) surface, the topmost layer is composed of La atoms as shown in Fig.7; no La atoms are located at the topmost layer of (111), and both the boron framework and the La atoms constructs the topmost structure of (110).

Figure 8 shows typical specular HREEL spectra of the (100), (110) and (111) surfaces. There is large difference in these spectra; the large peaks appeared at 16 and 27 meV, and the small peaks at 83, 122 and 162 mev in the spectrum of (111) while no peak was observed in the spectrum of (100). The (110) spectrum was the intermediate state between the (100) and (111) surfaces. The difference is explained from the known surface structures as shown in Fig.7. The conduction electrons are situated in the bands composed of d orbital of La atoms. The (100) surface is covered with the topmost La layer. Consequently, the conduction electrons covering the boron framework inevitably shields the dipole fields excited by the surface phonons. On the (111) surface, on the contrary, the fields are not shielded perfectly, because the boron frame work is situated out of the free electron sea. The (110) surface is the intermediate states of the shielding effects, which corresponds to the obserbed intermediate spectrum. The experimental data indicated that HREELS provides the new information about outermost electron distributions around the surface.

Figure 9 shows the observed dispersion curves of LaB_6 (100), and the corresponding theoretical curves, which are calculated based on a slab model with the same dynamical parameters as in bulk. The solid curves indicate the surface phonon modes. Adjusting carefully the surface force constants (SFC's) by several fitting procedures, we can reproduce the

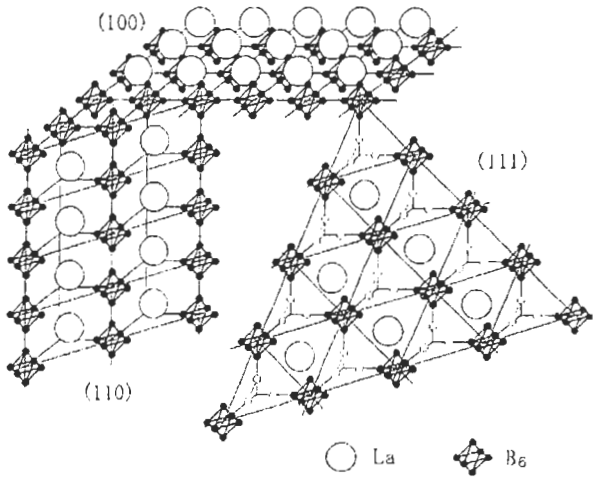

Fig. 7 Atomic structures of LaB_6 (100), (110) and (111) surfaces. The topmost layer of (100) is covered with La atoms, while boron framework is located at the topmost layer of (111).

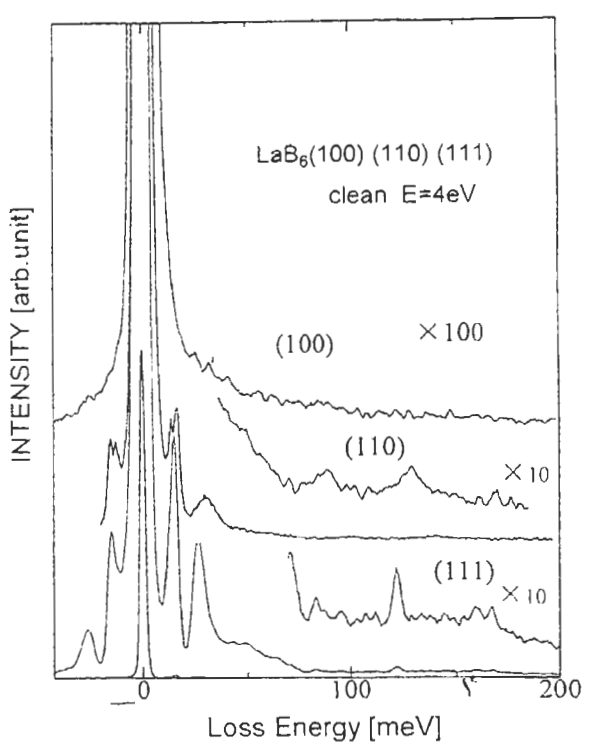

Fig. 8 The specular HREEL spectra of LaB_6 (100), (110) and (111) surfaces. We observed large loss peaks on the (111) surface and a tiny peak on the (100) surface.

prominent experimental loss peaks. The calculated dispersion which gives the best fit among the ~90 combinations in this calculation of the SFC's. Since the theoretical calculation explains well the measured dispersion curves without any assumption of drastic surface reconstruction such as breaking down of the octahedra, it is indicated that the B_6 octahedra:

It is consistent with the STM observation on LaB_6 (100) that revealed the step height to be 0.4 nm, which corresponds to the dimension of a unit cell. Comparison of the inter-octahedral SFC with bulk force constant has predicted the expansion of the octrahedra by about 0.004 nm parallel to the surface. In similar way, we found the shrinking of inter-octahedral bonds at the (111) surface, 0.007nm, during the analysis of the phonon dispersion.

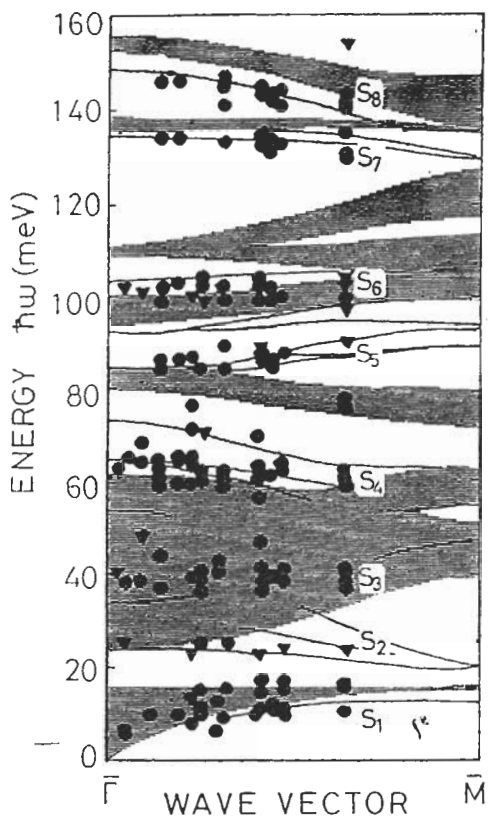

Fig. 9 Experimental dispersion curves of LaB_6 (100).

6. Conclusions

We have reviewed the recent data of HREELS. Slow electrons interact strongly with the dipole fields of the FK mode, resulting in large loss peaks. From the analysis of the FK mode, the atomic structure, and the thickness of Al_2O_3 thin layer were determined. In addition, we have demonstrated that the HREELS is a powerful tool to search the high frequency phonons of graphite, h-BN and LaB_6. The phonon dispersion curves of thin film and surfaces provide a large amount of information about chemical bonding and deformation of surface lattice.

Reference

1. H.Ibach and D.L. Mills, *Electron Energy Loss Spectroscopy and surface Vibrations*, Academic Press 1982.
2. W.Kress and F.W. de Wette, *Surface Phonons*, Springer-Verlag 1991.
3. C.Oshima, T.Aizawa, R.Souda, Y.Ishizawa and Y. Sumiyoshi, Solid State Commun. 65 (1988) 1601.
4. T.Nagao, Y. Iiizuka, M.Umeuchi, T.Shimazaki, M.Nakajima and C.Oshima, Rev. Sci. Instrum. 65 (1994)515.
5. H.Ibach J. of Electron Spectroscopy and related Phenomena, 64/65(1993) 819.
6. H.Ibach, Electron Energy loss Spectrometers, Springer Series in Optical Sciences 63, Springer, Berlin 1991 ISBN 3-540-528-0
7. Ph. Lambin, T.Laloyaux, P.A. Thiry, J.P. Vigneron and A.A. Lucas, Europhysics Letters, 2(1986)409 .
8. W.Kress, F.W. de Wette, A.D. Kulkarni, and U. Schroeder, Phys. Rev. B35(1987)5783.
9. W.Kress (Private Communications).
10. Gassmann, R.Franchy and H. Ibach, J. Electron Spectroscopy and Related Phenomena 64/65 (1993) 315.
11. C.Oshima and A. Nagashima, J. Phys: Condens. Matter. 9(1997) 1-19.
12. R.Niklow, N. Wakabayashi and F.G. Smith, Phys. Rev. B5 (1972) 4951.
13. R.J.Nenanich, G.Lucovky and S.A. Splin, Solid State Commun., 23 (1977)117.
14. T.Aizawa, R.Souda, S.Otani,Y.Ishizawa and C.Oshima, Phys. Rev.Lett. 64 (1990) 768.
15. A.Nagashima, N.Tejima, Y, Gamou, T. Kawai and C. Oshima, Surface Sci. 357/358 (1996)307.
16. E.Rokuta, Y.Hasegawa, S.Suzuki, and C.Oshima (Unpublished).
17. Y.Gamou, A.Nagashima, K.Terai and C.Oshima (Unpublished).
18. T.Nagao, K.Kitamura, Y.Iizuka, C.Oshima, and S.Otani, Surface Sci.290(1993)436.
19. E.Rokuta, N.Yamaoto, Y.Hasegawa, M.Trenary, T.Nagao, C.Oshima, and S.Otani, Surface Sci.357/358 (1996) 307.